# Lattice solitons in self-defocusing optical media: analytical solutions of the nonlinear Kronig–Penney model

**Y. Kominis and K. Hizanidis**

*School of Electrical and Computer Engineering, National Technical University of Athens, Zographou GR-15773, Greece*

Received May 23, 2006; accepted June 19, 2006;
posted July 10, 2006 (Doc. ID 71254); published September 11, 2006

A novel method for obtaining analytical solitary wave solutions of the nonlinear Kronig–Penney model in periodic photonic structures with self-defocusing nonlinearity is applied for providing generic families of solutions corresponding to the gaps of the linear band structure. Characteristic cases are shown to be quite robust under propagation. © 2006 Optical Society of America

*OCIS codes:* 190.4420, 130.2790, 190.5530.

Periodic photonic structures fabricated in nonlinear dielectric media recently became a subject of intense theoretical and experimental research. The formation of self-trapped localized modes, among others, is of major importance.[1,2] These modes have the form of gap solitons inside the photonic gaps of the periodic structure and result from the dynamical balancing between the nonlinearity and the diffraction. The robustness of these waves under propagation facilitates their experimental observation[3] and is very promising for applications in integrated photonic devices and waveguide arrays, such as multiport beam coupling, steering, and switching.[4–6] On the other hand, the related field of Bose–Einstein condensates loaded in optical lattices[7–11] is of increasing interest, and the theoretical studies in both fields progress in parallel.

The formation and propagation of localized modes in photonic structures have been theoretically studied mostly on the basis of either the tight-binding approximation or the coupled-mode theory rendering simplified discrete models.[12–16] These approximations provide accurate modeling only under the corresponding assumptions, while a more general model is the nonlinear Schrödinger equation (NLS) with spatially periodic coefficients

$$i\frac{\partial\psi}{\partial z}+\frac{\partial^2\psi}{\partial x^2}+\epsilon(x)\psi+g(x,|\psi|^2)\psi=0, \qquad (1)$$

where $z$, $x$, and $\psi$ are the normalized propagation distance, transverse dimension, and electric field, respectively. The periodic transverse variation of the linear refractive index is given by $\epsilon(x)$, while the spatial and intensity dependence of the nonlinear refractive index is provided through $g(x,|\psi|^2)$. This model has been previously studied for the case of the periodic function in the form of the periodic sequence of Dirac functions.[1,17] In recent work,[18] the case of a more realistic model with piecewise-constant coefficients, namely, a nonlinear Kronig–Penney model, has been considered, and a new method was utilized to provide analytical solutions for the case of a self-focusing nonlinearity. In this Letter, the same approach is applied for the case of self-defocusing nonlinearity (or repulsive interatomic interactions for the case of Bose–Einstein condensates). The analytical solutions thus obtained correspond to localized excitations on a finite periodic background in the form of dark and antidark solitons.

The stationary solutions of Eq. (1) have the form $\psi(x,z)=u(x;\beta)e^{i\beta z}$ and satisfy the nonlinear ordinary differential equation

$$\frac{d^2u}{dx^2}+[\epsilon(x)-\beta]u+g(x,u^2)u=0, \qquad (2)$$

where $\beta$ is the propagation constant and $u(x;\beta)$ is the real transverse wave profile. The periodic structure (Fig. 1) under consideration consists of linear and nonlinear (Kerr type) layers with the linear and the nonlinear refractive index given by $[\epsilon(x),g(x,u^2)]=(\epsilon_N,-2u^2)$, for $x\in U_N$ and $[\epsilon(x),g(x,u^2)]=(\epsilon_L,0)$ for $x\in U_L$, where $U_N=\cup_k(kT-N/2,kT+N/2)$; $U_L=\cup_k[kT+N/2,(k+1)T-N/2]$; $L$ and $N$ are the lengths of the linear and the nonlinear layers, respectively; and $T=L+N$ is the spatial period of the structure. In each part of the photonic structure the wave profile is described by the following equations:

$$\frac{d^2u}{dx^2}+(\epsilon_N-\beta)u-2u^3=0, \quad x\in U_N, \qquad (3)$$

$$\frac{d^2u}{dx^2}+(\epsilon_L-\beta)u=0, \quad x\in U_L. \qquad (4)$$

The stationary solutions of Eq. (2) can be provided by composing solutions of these two dynamical systems that have matched conditions for $u$ and its de-

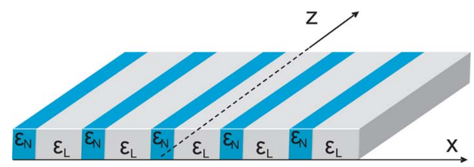


Fig. 1. (Color online) Geometry of the periodic structure consisting of linear ($\epsilon_L$) and nonlinear ($\epsilon_N$) layers.

 

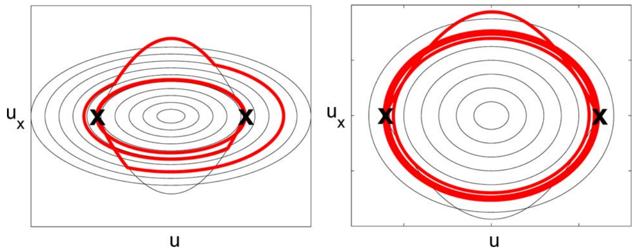


Fig. 2. (Color online) Phase space representation of the stationary solutions (thick curve) for the case of $n$, odd (left); and $n$, even (right). The phase space of the linear system (elliptic curves) and the heteroclinic orbit connecting the saddle points (x) of the nonlinear system, are shown.

rivative at the interfaces; a similar approach has been applied thus far only in cases with localized (nonperiodic) transverse inhomogeneity.[19,20] Furthermore, we assume that the propagation constant $\beta$ is such that (i) the linear system has periodic (sinusoidal) solutions, i.e., $\beta<\epsilon_L$, and (ii) the nonlinear system has a heteroclinic orbit $v(x;\beta,x_0) = \pm\sqrt{(\epsilon_N-\beta)/2}\tanh[\sqrt{(\epsilon_N-\beta)/2}(x-x_0)]$ connecting the saddle points $(u,u_x)=[\pm\sqrt{(\epsilon_N-\beta)/2},0]$, i.e., $\beta<\epsilon_N$. For a propagation constant corresponding to the case where an integer number of half-periods of the solution of the linear system is contained in the linear part of length $L$, i.e.,

$$\beta_n = \epsilon_L - (n\pi/L)^2, \quad n=1,2,\ldots, \tag{5}$$

any solution of Eq. (2), starting from a point of the heteroclinic orbit inside the nonlinear part at some $x$, returns to the heteroclinic orbit after evolving in the linear part; subsequently, it evolves again according to the heteroclinic orbit. Thus the solution tends asymptotically to the saddle points for $x\to\pm\infty$. The representation of the composite solutions in the phase space of the system $(u,u_x)$ is depicted in Fig. 2 for the case of an odd (even) $n$ where the solution lays on both (one of the) heteroclinic branches. *The localized stationary solutions corresponding to $\beta_n$ can be given analytically in the following form:* $u(x;\beta_n,x_0) = (-1)^{nk}\sqrt{(\epsilon_N-\beta_n)/2}\tanh[\sqrt{(\epsilon_N-\beta_n)/2}(x-x_0-kL)]$ for $x\in U_N$, $u(x;\beta_n,x_0)=a_k\sin(\sqrt{\epsilon_L-\beta_n}x+\phi_k)$ for $x\in U_L$, where $(a_k,\phi_k)$ are directly obtained from the continuity conditions of $u$ and its derivative at the interfaces. It is worth mentioning that, in contrast to the case of a self-focusing nonlinearity,[18] for the present case and for any parameter set there exists an infinite number of $\beta_n$'s, and solutions can be found for $\epsilon_L=\epsilon_N$, as well.

For each $\beta_n$ a family consisting of an infinite number of solutions parameterized by $x_0\in[-N/2,N/2]$ is obtained. Owing to the symmetry of the periodic structure the analysis is restricted to solutions with $x_0\in[0,N/2]$. The solutions are symmetric or antisymmetric with respect to the center of the nonlinear or the linear layer for $x_0=0$, $N/2$, respectively, while they are in general asymmetric for $x_0\neq 0,N/2$. In Fig. 3 several spatial profiles are shown for $x_0=0,N/2$ for the case of a periodic structure having $L=4\pi$, $N=\pi$, and $\epsilon_N=0$. For a $\Delta\epsilon\equiv\epsilon_L-\epsilon_N>0$ [Fig. 3 (left column)], one obtains dark solitary wave profiles formed as localized dips on a finite periodic background for $n=2$. For a negative $\Delta\epsilon$, antidark solitary wave profiles are obtained for $n=1$ [Fig. 3 (middle column)], while for $n=2$ the profile changes from (slightly) dark to antidark when $x_0$ increases from zero to $N/2$ [Fig. 3 (right column)]. A characteristic parameter for the form of a profile is the contrast $C$ with respect to the background. It is defined as the ratio between the maximum field value in the linear layer $x\in[N/2,N/2+L]$ to the absolute field value on a nonlinear layer for large $x$ [i.e., the saddle point of nonlinear system (4)]. It can be readily calculated analytically and its dependence on $x_0$ is shown in Fig. 4 (top row). It is shown that for the case $\Delta\epsilon=0.1$ only dark localized modes exist ($C<1$), while for $\Delta\epsilon=-0.5$ both dark ($C<1$) and antidark ($C>1$) modes exist. Note that in both configurations a dark solitary wave is formed for large $n$ and for values of $x_0$ close to $N/2$, while a $x_0$ close to zero results in $C=1$.

The location of the $\beta_n$ corresponding to analytical solutions in the linear band structure (propagation constant $\beta$ versus Bloch wavenumber $q$) of the system is depicted in Fig. 4 (bottom row) for $\Delta\epsilon=0.1$, $-0.5$. The band structure has been obtained by linearizing Eq. (3) around its fixed points (saddles). It is shown that all $\beta_n$ corresponding to solutions are located inside the gaps of the band structure. For the case of $\Delta\epsilon=0.1$, $\beta_1$ [as obtained from Eq. 5], does not fulfill the existence condition (ii) ($\beta<\epsilon_N$). It is noticeable that this value [marked as x in Fig. 4 (bottom row, left column)] is located within the linear transmission band where, in principle, solitary waves are not expected to exist.

The evolution of the stationary solutions (under the superposition of a random noise of $10^{-2}$ of the solution maximum), corresponding to Fig. 3 (top row, left column) and Fig. 3 (bottom row, middle column), is shown in Fig. 5. The stationary solutions undergo a robust evolution, which is quite promising for potential optical applications. For example, for a nonlinear material of AlGaAs type, when the transverse coordinate is normalized to $X=2$ to $3\ \mu$m, the normalized maximum propagation distance $z_{\max}=30$ corresponds

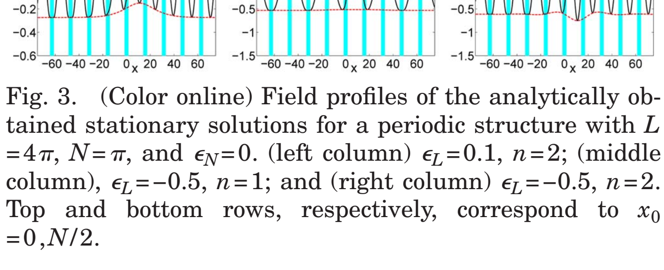

Fig. 3. (Color online) Field profiles of the analytically obtained stationary solutions for a periodic structure with $L=4\pi$, $N=\pi$, and $\epsilon_N=0$. (left column) $\epsilon_L=0.1$, $n=2$; (middle column), $\epsilon_L=-0.5$, $n=1$; and (right column) $\epsilon_L=-0.5$, $n=2$. Top and bottom rows, respectively, correspond to $x_0=0,N/2$.

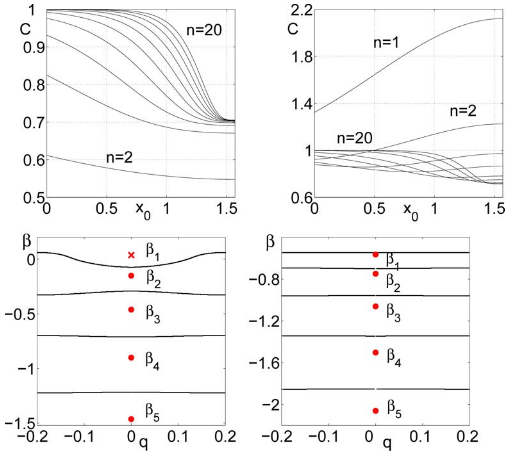


Fig. 4. (Color online) (Top row) Contrast versus $x_0$, and (bottom row) band structure (propagation constant $\beta$ versus Bloch wavenumber $q$) and location of the propagation constants $\beta_n$ of the analytically obtained stationary solutions (x: no analytical solution exists). The parameters are (left column) $L=4\pi$, $N=\pi$, $\epsilon_N=0$, and $\epsilon_L=0.1$; (right column) $\epsilon_L=-0.5$.

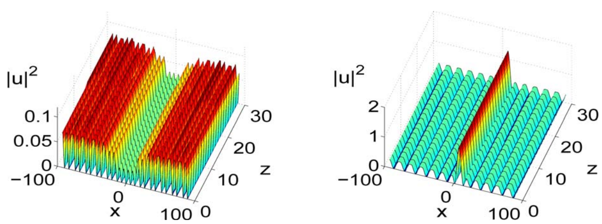


Fig. 5. (Color online) Propagation of the solitary waves corresponding to Fig. 3 (top row, left column) and Fig. 3 (bottom row, middle column) from left to right, respectively.

to an actual propagation length of 3.2–7.3 mm. It is worth mentioning that in such experimental configurations, even if some kind of instability occurs, the laminar propagation distance in several cases can be much larger than the actual length of the device. However, the complete stability characterization of each member of every family of solutions requires further analysis including the following issues: the stability of the background, the stability with respect to the parameters of the model, and the stability with respect to nearby solutions. The calculation of the complete linear spectrum for localized modes, such as those obtained in this work, presents significant difficulties.[21] It is a nontrivial problem except for some limiting cases where perturbation methods can be utilized. However, there exist results indicating that the linear spectrum of gap solitons, in general, includes a number of internal (discrete) modes[22] that may lead to persisting dynamics such as amplitude oscillations. On the other hand, a characteristic type of oscillatory instability, which has been identified in several 1D photonic structures, occurs when an internal mode crosses into a linear transmission band (shown in Fig. 4) and resonates with the linear Bloch waves. Such instabilities can trigger various types of spatial dynamics including symmetry breaking and oscillatory instabilities.[21,23–25] Numerical simulations show that the stability issue and the associated growth rate depend on the energy and the shape of the initial profile.

In conclusion, a novel method is applied for providing analytical solitary wave solutions in periodic photonic structures. These solutions form a generic family, corresponding to the gaps of the linear band structure, shown to be quite robust under propagation in several cases.

The project is funded by the joint Greek–European Union grant EPAEK II-PYTHAGORAS. K. Hizanidis's e-mail address is kyriakos@central.ntua.gr.

## References

1. A. A. Sukhorukov, Y. S. Kivshar, H. S. Eisenberg, and Y. Silberberg, IEEE J. Quantum Electron. **39**, 31 (2003).
2. J. W. Fleischer, G. Bartal, O. Cohen, T. Schwartz, O. Manela, B. Freedman, M. Segev, H. Buljan, and N. K. Efremidis, Opt. Express **13**, 1780 (2005).
3. D. Mandelik, R. Morandotti, J. S. Aitchison, and Y. Silberberg, Phys. Rev. Lett. **92**, 093904 (2004).
4. R. A. Vicencio, M. I. Molina, and Y. S. Kivshar, Opt. Lett. **28**, 1942 (2003).
5. R. A. Vicencio, M. I. Molina, and Y. S. Kivshar, Opt. Lett. **29**, 2905 (2004).
6. Y. V. Kartashov, L. Torner, and V. A. Vysloukh, Opt. Lett. **29**, 1102 (2004).
7. F. Kh. Abdullaev, B. B. Baizakov, S. A. Darmanyan, V. V. Konotop, and M. Salerno, Phys. Rev. A **64**, 043606 (2001).
8. G. L. Alfimov, V. V. Konotop, and M. Salerno, Europhys. Lett. **58**, 7 (2002).
9. V. V. Konotop and M. Salerno, Phys. Rev. A **65**, 021602(R) (2002).
10. N. K. Efremidis and D. N. Christodoulides, Phys. Rev. A **67**, 063608 (2003).
11. P. J. Y. Louis, E. A. Ostrovskaya, and Y. S. Kivshar, J. Opt. B **6**, S309 (2004).
12. Y. S. Kivshar, W. Krolikowski, and O. A. Chubykalo, Phys. Rev. E **50**, 5020 (1994).
13. M. Johansson and Y. S. Kivshar, Phys. Rev. Lett. **82**, 85 (1999).
14. V. V. Konotop and S. Takeno, Phys. Rev. E **60**, 1001 (1999).
15. B. Sanchez-Rey and M. Johansson, Phys. Rev. E **71**, 036627 (2005).
16. H. Susanto and M. Johansson, Phys. Rev. E **72**, 016605 (2005).
17. S. Theodorakis and E. Leontidis, J. Phys. A **30**, 4835 (1997).
18. Y. Kominis, Phys. Rev. E **73**, 066619 (2006).
19. C. K. R. T Jones, T. Kupper, and K. Schaffner, Z. Angew. Math. Phys. **52**, 859 (2001).
20. R. K. Jackson and M. I. Weinstein, J. Stat. Phys. **116**, 881 (2004).
21. P. J. Y. Louis, E. A. Ostrovskaya, C. M. Savage, and Y. S. Kivshar, Phys. Rev. A **67**, 013602 (2003).
22. Y. S. Kivshar, D. E. Pelinovsky, T. Cretegny, M. Peyrard, Phys. Rev. Lett. **80**, 5032 (1998).
23. A. A. Sukhorukov and Y. S. Kivshar, Phys. Rev. Lett. **87**, 083901 (2001).
24. D. E. Pelinovsky, A. A. Sukhorukov, and Y. S. Kivshar, Phys. Rev. E **70**, 036618 (2004).
25. J. Yang and Z. Chen, Phys. Rev. E **73**, 026609 (2006).